



Valorising excavated low-grade waste clay in limestone calcined clay cement system for 3D printing applications

Yazeed A. Al-Noaimat^a, Mehdi Chougan^b, Eslam El-Seidy^a, Abdulrahman Albar^c, Seyed Hamidreza Ghaffar^{d,e,*}

^a Department of Civil and Environmental Engineering, Brunel University, Uxbridge, Middlesex, London, UB8 3PH, United Kingdom

^b School of Mechanical, Aerospace and Civil Engineering, The University of Sheffield, Sheffield, S1 3JD, United Kingdom

^c Bina Robotics Ltd. CRL, Shipping Building, 252 Blyth Rd., Hayes, UB3 1HA, United Kingdom

^d Department of Civil Engineering, University of Birmingham, Dubai International Academic City, P.O. Box 341799, Dubai, United Arab Emirates

^e Applied Science Research Center, Applied Science Private University, Jordan

ABSTRACT

Limestone calcined clay cement (LC3) presents a suitable low-carbon cementitious material for large-scale 3D printing due to its long open time. This study investigates the impact of substituting up to 100 % natural aggregate with recycled brick aggregates (BA) on the engineering properties, durability and printing properties of LC3. BA's rough surface and irregular shape reduced the workability of the LC3 mixtures even though the water absorption of BA was compensated for by adding extra water. The mechanical strength increased significantly in the presence of BA of around 36 %–62 %. Moreover, incorporating BA was found to boost the hydration and allowed it continue due to the presence of additional water in its microstructure. The water absorptions of LC3 prepared with up to 70 % replacement level of aggregates with BA were comparable to the reference mix, while a 100 % replacement level increased the water absorption by around 9 %. In contrast, incorporating BA improved the freeze-thaw resistivity by up to 25 %. Moreover, it was found that incorporating BA improved the layer quality of 3D-printed filaments. The results of this study present a breakthrough in the recycling of brick aggregates in LC3 systems for both cast and 3D printing applications, which will help develop a more environmentally friendly mixture with high engineering performance.

1. Introduction

The most widely used manmade material in the world is concrete, and it is a key material to meet the demand for rapid development and maintenance in the construction sector [1–3]. Over 4 billion tonnes of ordinary Portland cement (OPC), the main ingredient of concrete, was reported to be produced yearly. This, in turn, has brought up major environmental concerns since OPC production is responsible for around up to 8 % of global CO₂ emissions [4–6]. The CO₂ emission related to processing OPC was reported to be 1.57 GT in 2019 [7], whereas it rose to nearly 2.9 Gt in 2021 [8]. To mitigate this issue, limestone calcined clay cement (LC3) has been developed as a sustainable solution, which allows the replacement of high percentages of OPC with calcined clay and limestone to produce a ternary blended cement [9]. The most commonly introduced clay mineral in calcined clay as a supplementary cementitious material (SCM) is kaolinite because of its high pozzolanic reactivity [10]. However, reserves for high-grade kaolinite clay are limited and the exploitation of this material in manufacturing different products would challenge its use as SCM in the near future [11–13]. Thus, the research has been moving towards studying the feasibility of utilising low-grade clay with low kaolinite content or various clay minerals [14,15]. Recently, Kanavaris et al. [16] investigated the suitability of repurposing excavated clays from a

* Corresponding author. Department of Civil Engineering, University of Birmingham, Dubai International Academic City, P.O. Box 341799, Dubai, United Arab Emirates.

E-mail address: S.h.Ghaffar@bham.ac.uk (S.H. Ghaffar).

<https://doi.org/10.1016/j.job.2025.112634>

Received 9 December 2024; Received in revised form 1 April 2025; Accepted 8 April 2025

Available online 12 April 2025

2352-7102/Crown Copyright © 2025 Published by Elsevier Ltd. This is an open access article under the CC BY license (<http://creativecommons.org/licenses/by/4.0/>).

tunnelling project (with around 18–22 % kaolinite content) in London as calcined clay to develop an LC3 mixture. The authors found that excavated clay can be used to develop LC3 mortars for structural purposes with a strength of 50 MPa.

Another impact of the rapid development of the construction industry is the over-exploitation of natural aggregate resources. In 2014 alone, the estimated consumption of aggregates was around 40.2 billion metric tonnes worldwide, increasing at a rate of 5.2 % yearly. A suitable approach that has received research interest in recent years is recycling wastes and employing them in new constructions. Waste materials, including construction and demolition waste (CDW) [17], rubber [18,19], and plastic wastes [20], were identified to be suitable for use as natural aggregate replacements in cementitious mixtures. This would decrease the over-reliance on limited natural resources and the problems associated with waste treatment and disposal. Up-to-date, many studies have been conducted to investigate the effect of incorporating brick waste in aggregate form, which is known to be the second major waste from CDW after concrete waste, to replace natural sand in cementitious mixtures [21–23]. Nevertheless, its porous microstructure and high water absorption are challenging its development as a construction material [24]. Although incorporating brick aggregates (BA) had a negative impact on the workability and some durability aspects of the cementitious mixtures [25], it was also reported to have a positive influence on the cementitious mixtures’ durability and enhanced cementitious mixtures’ mechanical properties [25–27]. Most recently, Huang et al. [22] investigated the effect of replacing up to 100 % of fine aggregates by volume with pre-soaked and dry BA on the properties of cement mortar. The authors found that the strength performance of cement mortar increased with dry BA replacement level while decreased when incorporating pre-soaked BA. In addition, the water absorption of the mortars decreased when incorporating dry BA and increased in the presence of pre-soaked BA [22]. Ge et al. [28] investigated the effect of replacing fine NA with fine BA up to 100 % by weight and examined the impact of pre-wetting fine BA for different time intervals (0, 0.5 and 24 h). Replacing NA with BA decreased the strength performance of mortar. However, pre-wetting the aggregates to longer time intervals reduced the extent of this strength loss. Moreover, incorporating BA and pre-wetting of BA decreased the drying shrinkage of mortar. The effect of BA on limiting shrinkage makes it beneficial for 3D printing applications since cementitious mixtures are susceptible to water evaporation in 3D printing leading to plastic and drying shrinkage due to formwork absence [29]. Nevertheless, many outstanding questions about the pros and cons of incorporating recycled BA in cementitious mixture remain and many gaps should be investigated.

In recent years, Olofinnade and Ogara [30] investigated the impact of substituting up to 50 % natural sand by weight with recycled BA on the properties of calcined clay blended cement and reported the strength to slightly increase when replacing up to 20 % while decreasing when incorporating more BA. Although some studies have investigated the impact of incorporating brick aggregate on

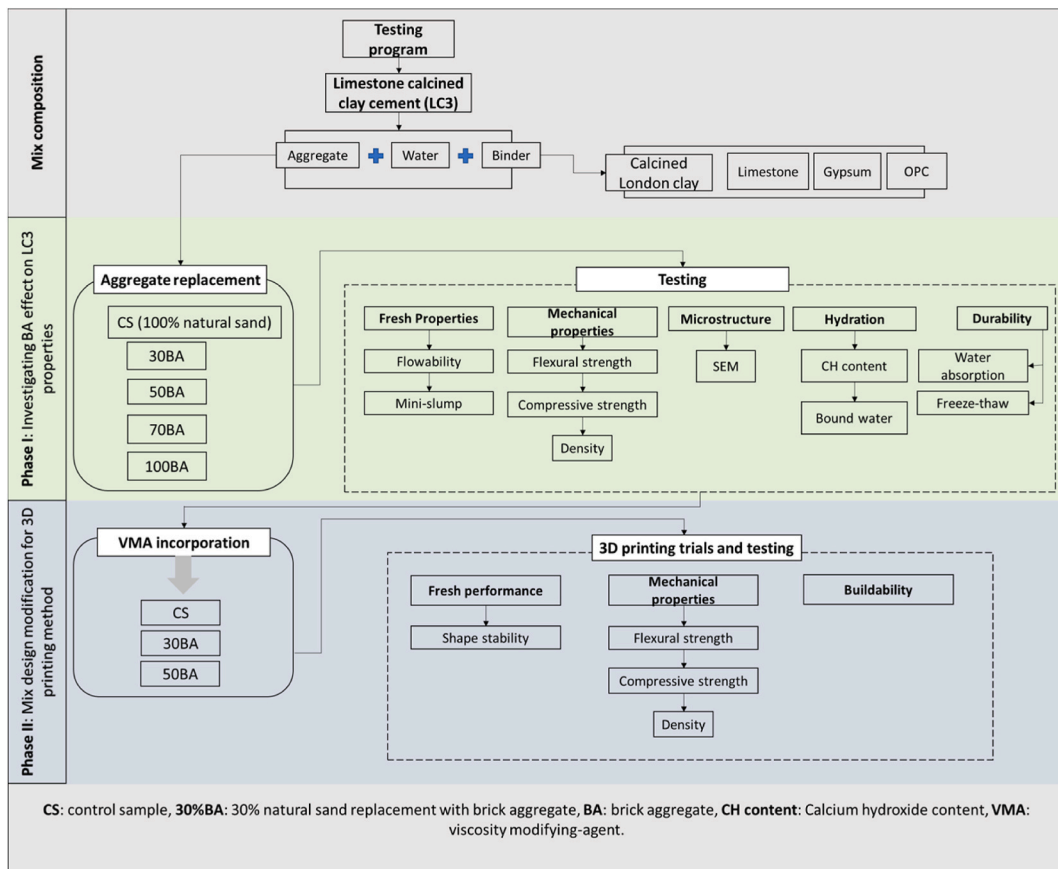


Fig. 1. Schematic overview plan of the experimental testing program.

different cementitious mixture properties, to the best of the authors' knowledge, there has been no research to investigate the influence of utilising brick aggregate on the properties of LC3 mixtures, especially those made of calcined excavated clay. This study addresses critical challenges faced by both local and global industries by investigating the potential for substituting up to 100 % of natural aggregates with brick aggregate in LC3 mixtures made with excavated London clay as calcined clay. First, the reuse of excavated clay aligns with circular economy principles, offering a sustainable alternative to the high environmental costs of sourcing virgin materials. Simultaneously, using brick aggregate diverts significant construction waste from landfills, addressing local waste management issues while providing an alternative aggregate to reduce the excessive reliance on limited natural sand. This study also investigates the suitability and impact of using brick aggregate on the strength properties and extruded filament quality of 3D printed LC3. This work considers compensating for brick aggregates' water absorption capacity by adding additional water to the mix design, considering the hypothesis that brick aggregates would work as an internal curing agent in the mixture. Furthermore, the novelty of this research is in quantifying and qualifying the benefits of utilising brick aggregate instead of natural aggregates on the properties of LC3 mixtures for cast and 3D printing methods. This in turn contributes to limiting the amounts of brick waste being landfilled or downcycled. Moreover, decreasing the overdependency on limited natural resources, i.e., natural aggregates. This study analyses the effect of substituting 30, 50, 70 and 100 % natural aggregates with brick aggregates on the fresh, hardened, durability and printing properties of the LC3 mixture.

2. Materials and methodology

Fig. 1 illustrates an overview plan of the experimental program.

2.1. Materials

This study used a commercial OPC (CEM I 52.5 N) from CEMEX, UK, in accordance with BS EN 197-1 [31]. A limestone powder of 99 % calcium carbonate purity from Normin Industrial Minerals, Oman, and gypsum from British Gypsum, saint-gobain, UK, were used. Excavated London clay (with 16.8 % kaolinite content) sourced from the HS2 project was used in this study as calcined clay. The chemical, mineralogical, and particle size distribution of the different binder materials, and the processing and calcination process of London clay to produce calcined London clay (CLC) can be found in the following reference, from the author's previous research. The optimum calcination temperature was determined based on the authors' previous study, where the ideal calcination temperature was 800 °C for 1h. Sika® ViscoCrete® 510 P polycarboxylate (Sika, Germany) was utilised as a superplasticiser (SP). A hydroxypropyl methylcellulose (HPMC)-based viscosity-modifying agent (VMA) was supplied from Alfa Aesar, USA. Siliceous river sand as natural aggregates (NA) certified by the supplier to use in concrete according to BS EN 12620:2013 [32] with particle size less than 2 mm was used. The brick aggregate (BA) was obtained through crushing waste brick collected from a demolition site near Brunel University London using a 100-grinder machine, Retsch, Germany, equipped with a 2 mm sieve, followed by sieving to obtain particles between 0.25 and 2 mm size to be used as recycled aggregate. The particle size of BA particles was limited to 0.25 mm to prevent it from participating in the binder reaction through its pozzolanic reaction and acting as inert filler [33]. More details about the used BA can be found in Refs. [4,6]. Sieve analysis was used to determine the particle size distribution of NA and BA and the curves are presented in Fig. 2. NA curve showed that around 25 % of the particles were between 1 and 2 mm and around 50 % passed the 0.5 mm sieve. On the other hand, BA had around 82 % of the particles retained above 1 mm sieve while the rest of the particles retained on 0.5 mm sieve. More details about the aggregates' characteristics and particle sizes can be found in Ref. [6].

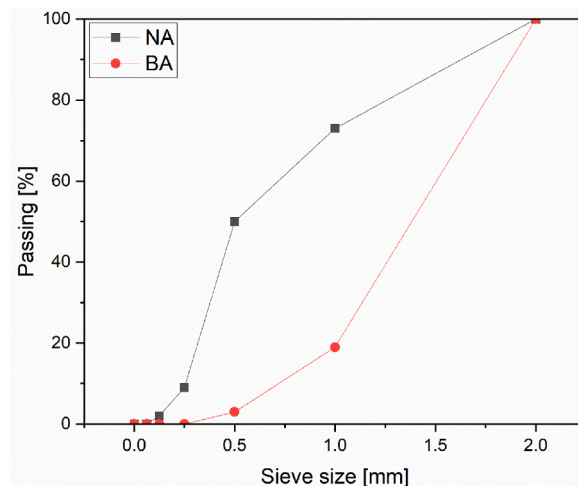


Fig. 2. Particle size distribution curves of NA and BA.

2.2. Mix formulations and sample preparation

A total of five different mix formulations were used in this study to investigate the effect of incorporating BA to replace NA in the LC3 mixture, which are presented in Table 1. The mix formulation used as the reference in this study was selected based on the authors' previous work on LC3 mixtures, which had the best-performing mechanical strength and printability performance. The binder composition was consistent across all mixtures, with 50 % OPC replacement, 30 % CLC, 15 % limestone (maintaining a CLC/limestone ratio of 2:1), and 5 % gypsum. The superplasticizer (SP) was fixed at 1 % by binder weight for all mixtures. An aggregate/binder ratio of 1.5 was used for all mixtures. The replacement levels of NA with BA used were 30, 50, 70 and 100 % by weight. The water absorption of the same BA was investigated in the authors' previous study [6] and was found to be 8.7 %. This value is significantly higher than that of sand at 0.5 %. Although, it was reported that incorporating dry recycled brick aggregate without considering to compensate for their water absorption improves the properties of the cementitious mixture [22], this study considered adding extra water to compensate for the water absorption of BA particles. Even though, it was reported that counting BA's water absorption would degrade cementitious mixture's behaviour [34], it might behave differently in LC3 since calcined clay's later age reactivity is influenced by the mixtures' internal relative humidity [3,35]. When incorporating additional water, BA absorbs water in its porous structure and starts releasing it slowly while the LC3 mixture continues to age [36], working as an internal curing agent by providing extra internal moisture that enables the mixture's hydration to elongate. Therefore, this study considered adding extra water to compensate for BA's water absorption as a hypothesis that it will be released to allow the hydration to proceed.

For 3D printing LC3 mixtures with different BA content, an HPMC-based VMA was incorporated into the mixtures to modify their viscosity, cohesion, and water-retention properties. The compatibility of cellulose-based VMA with polycarboxylate (PCE)-based superplasticiser has been reported in previous studies [37,38]. However, when PCE and HPMC are presented together in the mixture, their competitive adsorption in the suspension cannot be avoided. The VMA dosage chosen for each mix was the minimum amount needed to facilitate the extrusion process while still enabling the mixture to retain its shape. The dosage was added based on the initial weight of the binder.

The LC3 mixtures with and without BA were prepared by dry mixing solid ingredients (OPC, CLC, LP, gypsum, SP, NA and BA) for 3 min in a Kenwood mortar mixer (Germany). Followed by gradually pouring the required amount of mixing water, including the water absorption of BA particles, and wet mixing for 5 min. For mixtures prepared with VMA, for 3D printing, VMA was added to the fresh mixture at the end of the 5 min wet-mixing process with SP, and the mixing continued for an additional 3 min. Mixtures were cast in prismatic polystyrene moulds at the end of the mixing process with a dimension of $40 \times 40 \times 160 \text{ mm}^3$ or fed to the printer for extrusion and cured in control room conditions at 40 % relative humidity and $20 \pm 3^\circ\text{C}$ for 24 h. The cast and extruded specimens were immersed then in a controlled water tank at $20 \pm 3^\circ\text{C}$ until test age.

2.3. 3D printing process

The 3D printing of the modified mixtures was conducted using a three-axis gantry-type extrusion-based 3D printer equipped with a custom-designed auger extruder, as shown in Fig. 3, consistent with a previous study conducted by the authors [39]. The samples were printed using a 20 mm circular-shaped nozzle with a motion speed of 15 mm/s and a 10 mm nozzle standoff distance.

2.4. Experimental methods

2.4.1. Workability

The effect of brick aggregate incorporation on the workability of the different mixtures was investigated by conducting a flow table test in accordance with BS EN 1015:3-1999 [40]. The flowability was determined instantly after the end of mixing and was calculated as the average flow spread diameter in two perpendicular directions.

To further investigate the impact of brick aggregates on the mixture's workability, a mini-slump test was conducted to determine the slump value of the different mixtures. The flow height reduction was measured at the end of the mixing process after pouring the mixture into the cone for 1 min and recorded as the slump value.

Table 1
LC3 mix formulations with and without BA.

Mix	Binder (%)				Aggregates (%)		Extra water (g)	Total W/b ratio	Effective W/b ratio
	OPC	CLC	LP	Gypsum	NA	BA			
0BA	50	30	15	5	100	–	–	0.3	0.3
30BA	50	30	15	5	70	30	25.2	0.34	0.3
50BA	50	30	15	5	50	50	42	0.36	0.3
70BA	50	30	15	5	30	70	58.8	0.38	0.3
100BA	50	30	15	5	–	100	84	0.42	0.3

*1 % SP by weight of binder was considered for all mixtures.

*A water-to-binder ratio of 0.3 was considered for all mixtures.



Fig. 3. Extrusion-based 3D printer (Bina Robotics).

2.4.2. Mechanical properties

Flexural strength (3-point bending) and compressive strength performances of the different mixtures were investigated at 7 and 28 days using a Universal Testing System (Instron 5960) following the procedures described in BS EN 196-1 [41] at a loading rate of 1 mm/min. More details and configuration for the different tests can be found in Ref. [42]. The tests were performed on cast samples with a dimension of $40 \times 40 \times 160 \text{ mm}^3$. For 3D printed samples' strength evaluation, straight lines with $40 \times 40 \text{ mm}^2$ cross-sections were 3D printed, as shown in Fig. 4, and specimens with a similar dimension to cast samples were extracted. The cut printed samples' dimensions were measured before testing to ensure accurate calculation of results. The results were calculated as the average of three and six sample recordings for flexural and compressive strength, respectively.

2.4.3. Microstructure analysis

Scanning electron microscopy (SEM) was used to study the microstructure of the LC3 mixtures with different brick aggregate content using a Supra 35VP device (Carl Zeiss, Germany). Small portions were collected after mechanical testing with an approximate dimension of 1 cm^3 for the analysis, oven-dried and gold-coated (Edwards S150B sputter coater) to prevent surface charging effects. To ensure meaningful observation, around 10 SEM images were captured for each sample at an accelerating voltage of 5 kV.

2.4.4. Thermogravimetric analysis

The reaction kinetics of the different mortars were investigated by determining Portlandite content using Thermogravimetric analysis (TGA). TGA was performed on mortar powder using an SDT Q600 instrument with a heating rate of $10 \text{ }^\circ\text{C}/\text{min}$ from $30 \text{ }^\circ\text{C}$ to $900 \text{ }^\circ\text{C}$. To do so, LC3 mortars with and without aggregates were mixed and cured similar to the procedures mentioned earlier. After 28 days, the different mixtures were crushed and ground. The grounded product was then sieved using a $63.5 \text{ }\mu\text{m}$ sieve. The total calcium hydroxide (Portlandite) content on the grounded powder was determined after 28 days from the mass loss in the temperature range of $400\text{--}500 \text{ }^\circ\text{C}$, which is attributed to the portlandite dehydration, with including the mass loss at the temperature range of $600\text{--}800 \text{ }^\circ\text{C}$,



Fig. 4. 3D printed line for extracting prismatic samples for mechanical strength evaluation.

which is assigned to the decomposition of calcium hydroxide that undergone carbonation and transformed into calcium carbonate. The following equation was used to calculate the total calcium hydroxide content in the different mixtures [22]:

$$CH \text{ content} = \frac{74}{18} \times WL_{CH} + \frac{74}{44} \times WL_{CC} \quad (\text{Eq. 1})$$

Where CH represents calcium hydroxide, WL_{CH} and WL_{CC} represent the percentage of weight loss by the dehydration of calcium hydroxide (CH) and calcium carbonate (CC), respectively.

2.4.5. Water absorption

The durability performance of the various mixtures was assessed by determining their water absorption. Water absorption was conducted following BS 1881-122:2011 [43] on prismatic cast specimens ($40 \times 40 \times 160 \text{ mm}^3$) cured for 28 days in water. Prior to testing, the specimens were oven-dried at 105C until reaching a constant mass, followed by weight recording and submerging in water. The mass of the submerged specimens was measured periodically for up to 72 h. The water absorption percentage was calculated using the equation below.

$$\text{Water absorption (\%)} = \frac{M_t - M_0}{M_0} \times 100 \quad (\text{Eq. 3})$$

Where M_t (g) represents the sample mass at time t after exposure to water, and M_0 (g) represents the oven-dried mass.

2.4.6. Freeze-thaw resistivity

The durability was also assessed by determining the freeze-thaw resistance of the different samples. The test was conducted on prismatic cast samples water-cured for 28 days in accordance with the Polish standard PN-85-B04500 [44]. The specimens were taken out from the water tank at the age of 28 days and placed inside the freeze-thaw chamber for 25 cycles. Each cycle involved 4 h of freezing at -20C , followed by 4 h of thawing at 20C at 98 % RH. Following the freeze-thaw cycles, a compressive strength test was performed, and the strength reduction was calculated using the following equation:

$$\text{Strength reduction (\%)} = \frac{C_1}{C_0} \times 100 - 100 \quad (\text{Eq. 4})$$

Where C_0 is the compressive strength of the normal cured mixture and C_1 is the compressive strength of the mixture after exposure to the FT cycles.

2.4.7. Buildability and filaments quality investigation

An ad-hoc testing method of 3D printing cylindrical objects was used to investigate the buildability of the different mix formulations with and without BA. The cylinders were printed with a 150 mm diameter and using a fixed amount of material, consisting of four batches of each mix, which makes around 8000 g of fresh mixture. The buildability of the mixtures was evaluated by investigating layer deformation and radial or vertical distortions. In addition, the final height of the printed object was assessed to the theoretically designed height from the computer model.

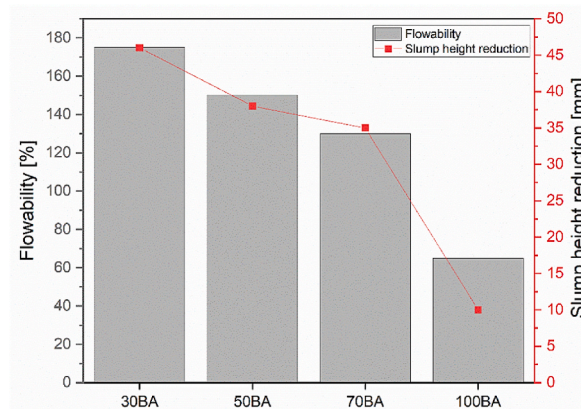


Fig. 5. Flowability and slump height reduction of LC3 mixtures containing BA.

3. Results and discussions

3.1. Effect of incorporating brick aggregates on LC3 properties

3.1.1. Fresh properties

Fig. 5 presents the flowability percentage and slump height reduction of the different mixtures content as an indication of the workability of the mix. The LC3 mixture prepared with NA had an excessive spread diameter greater than the mini-slump table diameter. Therefore, it wasn't presented in the bar graph results and was considered greater than 290 mm (>190 %), which is the diameter of the mini-slump table. The workability of the mixtures decreased with increasing the replacement level in LC3 mixtures. For instance, increasing the replacement level of aggregates from 30 % to 50 % reduced the flowability by 25 %, reaching 150 % from 175 %. The workability and fresh properties of the cementitious mixture are significantly affected by the aggregate's characteristics, including size, shape and surface texture [45]. The BA used in this study exhibits a water absorption capacity of 8.7 % determined following the procedures in BS EN 12620:2013 [32]. Depending on BA'S raw materials and production process, its porosity and water absorption can be as high as 40 % [36]. Even though the water absorption of BA was compensated for in the mix design, the workability still decreased. This is mainly due to BA's geometry and surface texture compared to NA's. BA particles have irregular and elongated shapes with a rough surface texture, which increases the friction between the different ingredients in the mixture and resistance to flow, which, in turn, significantly declines the workability. This effect is significant when increasing the replacement level from 70 % to 100 %, which exhibited a significant drop in workability, reaching a flowability of 65 % from 130 % and a slump height reduction of 10 mm from 30 mm. That is because of the complete replacement of NA with spherical and round particles that act as rollers and improve the flow of the mixtures with BA particles that have a rough and irregular structure which hinders the flowability of the mix.

3.1.2. Mechanical strength

Flexural and compressive strength performances of the mixtures prepared with different BA content were investigated at 7 and 28 days, and the results are presented in Fig. 6. An evident progressive increase can be observed in strength results when the replacement level of NA with BA is increased. Fig. 6a shows that LC3 mixtures with BA achieved 22–87 % and 8–36 % better flexural strength performance than the reference mixture at 7 and 28 days, respectively. Similarly, compressive strength results showed around 20–87 % and 36–62 % higher results than the reference mixture after 7 and 28 days, respectively, as shown in Fig. 6b. The highest flexural strength was reported for the LC3 mixture with 100 % BA, which achieved 12.5 MPa, whereas compressive strength was found to be comparable for mixtures with replacement levels of 50 % and above, reaching around 54 MPa, which is higher than the natural sand and 30BA mixes. Previous studies showed contradictory behaviour for incorporating BA to replace NA in cementitious mixtures [46, 47]. For instance, Zhang et al. [47] showed that incorporating 30 % BA decreased the compressive strength of concrete by around 18 %. According to Zhang et al. [47], the reduction in strength performance was related to BA's weaker crushing index than NA's. It should be noted that the authors considered adding extra water to compensate for the water absorption of BA. Bektas et al. [36] reported similar strength behaviour when replacing natural sand by up to 20 % in cement mortar. However, the authors didn't consider compensating for the water absorption of BA in the mix design. Some studies considered compensating BA particles' water absorption by adding extra water or soaking BA in water until saturation [22,28], while others did not consider compensating for the water being absorbed [30]. Huang et al. [22] considered comparing the effect of replacing NA up to 100 % with BA in two conditions (dry state and after pre-soaking in water) on cement mortars' performance and found that using BA in a dry state enhanced the strength performance of the mortars compared to that of pre-soaked BA which declined the properties of the mortar. The authors reported around 20 % and 80 % higher strength for flexural and compressive strength, respectively than the mixture prepared with NA. That is in good agreement with the results presented in this study, however, this study considered compensating for BA's water absorption. According to Briki et al. [35], chemical shrinkage progressively empties the capillary pores after setting, decreasing the internal relative humidity of the

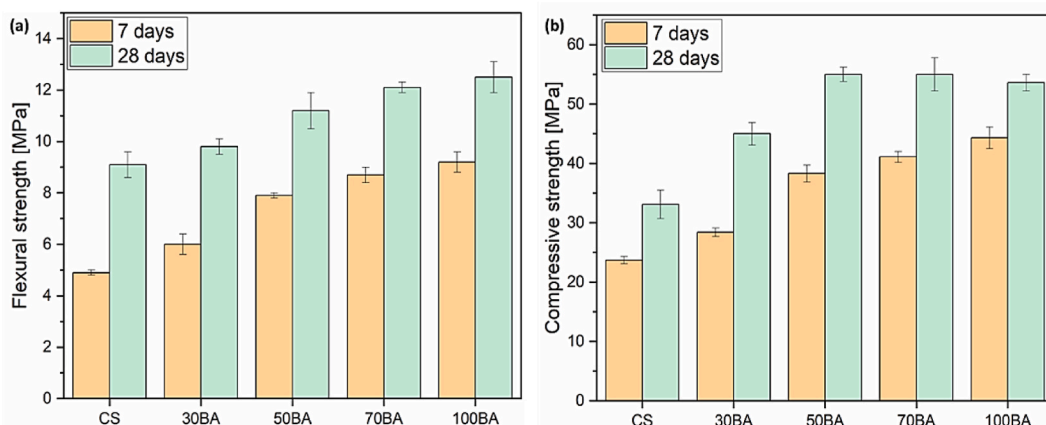


Fig. 6. (a) Flexural and (b) compressive strength of the different LC3 mixtures after 7 and 28 days.

mixture. That, in turn, slows down the calcined clay reaction rapidly after 7 days. The authors found that calcined clay's reaction increases with increasing water content or the saturation level of capillary pores. However, this improvement in reaction would slow down after 28 days, even in the presence of more solution in the capillary pores [35]. According to Ge et al. [28], incorporating BA in cementitious mixtures decreased the internal humidity loss over time. Moreover, pre-wetting BA was found to further slow the internal relative humidity loss over time by transferring the water from BA to the cementitious matrix with ageing. Hence, in this study, the inclusion of extra water to compensate for BA's water absorption may not have changed the saturation level of the fresh mixture since BA would absorb the excessive water from the fresh mixture (around 4–12 % to the binder weight for the different replacement levels). Nevertheless, BA particles might reduce the loss in internal relative humidity with ageing through releasing some of the water being held in their microstructure. Consequently, LC3 mixtures prepared with different BA content contain additional water, which could participate in LC3's hydration and reaction at later ages. That allows BA to work as an internal curing agent during ageing by releasing some of the initially absorbed water during self-desiccation, allowing the hydration to continue and the production of more densified and compacted microstructure. Moreover, if the water remained inside the BA particles and was not used for cement hydration, it would make the BA particles denser by filling the pores [46]. These previous observations and explanations could explain the higher strength development of LC3 mixtures prepared with BA than that of NA in this study.

The aggregates' characteristics, such as textural and physical properties, also affect the cementitious mixtures' mechanical strength [48]. Another reason for the improvement of mechanical strength in the presence of BA could be the particle's porous and rough texture and irregular shape, which could enhance the bond and adhesion between the aggregates and the matrix. That was confirmed by SEM images, as shown in Fig. 7, which shows that BA particles are entirely and perfectly (i.e., without any delamination) embedded in the microstructure of the LC3, having a good bonding with the paste without showing debonding at the interface between the aggregates and matrix. The strong adhesion of the BA and its effective interlocking with the cement paste play an important role in improving the overall mechanical performance. When the cementitious mixture is subjected to external loading, the strong adhesion and interlocking mechanisms allow for the efficient stress transfer between the paste and BA, contributing to the material's improved mechanical strength behaviour. Moreover, the strength improvement could be related to the higher content of larger particles in BA particle size distribution ($d_{50} < 1.4$ mm) than NA ($d_{50} < 0.5$ mm), as shown in Fig. 2, since it is well-established that compression resistivity of the cementitious mixture increases with increasing aggregates' particle size distribution [6,49].

The effect of BA incorporation on the LC3 hydration was investigated by determining the amount of hydration products as a means of calcium hydroxide (CH) content and by calculating the bound water content. Huang et al. [22] determined the impact of incorporating BA on the hydration of cement by calculating the mass loss associated with CH using TGA curves as the total mass loss from CH dehydration and calcium carbonate (CaCO_3) decarbonation. Similarly, in this study, the total CH content (%) in the powdered mortars was calculated as the summation of CH dehydration percentage and calcium carbonate decarbonation, and the results are presented in Table 2. It can be observed that the CH content increased in the presence of BA. This is due to the internal curing effect of BA, which promoted the continuous hydration of the mixtures and allowed the production of additional portlandite and hydration products. Nevertheless, CH content decreased with increasing BA content in the LC3 mix from 30 % onwards. This could indicate that incorporating 30 % BA while accounting for their water absorption was sufficient to allow the unreacted cement particles to react and produce additional CH. According to Sun et al. [50], the presence of additional CH was found to enhance the reaction of calcined clay and promote the formation of carboaluminates, which contributes to improving the mechanical strength of the mixture. Moreover, aluminate presented in calcined clay could also react with calcium hydroxide to produce Ettringite (Aft) and monosulfate phases [51]. This could indicate the consumption of CH in the reaction to produce more hydration products, which might explain the significant strength performance improvement in the mixtures containing BA. Huang et al. [22] reported that BA incorporation promotes continuous hydration through its internal curing effect in the mix and increases the CH content in the mixture. It should be noted that the authors investigated the effect of BA on plain OPC mortar, which explains the reason behind the higher CH content in their study in the presence of BA. Hence, in this study, the internal curing effect in the presence of BA allows the continuous pozzolanic reaction of calcined clay and limestone with CH and the production of more hydration products since calcined clay reactivity is influenced by the internal relative humidity and the presence of CH [35]. Hence, the decrease in CH content with BA content suggests a better pozzolanic reaction, and the formation of more hydration products, which could be another added explanation for the better mechanical strength of the mixtures. Moreover, despite BA's large particle size, their high silica and aluminate content could allow their surface to provide

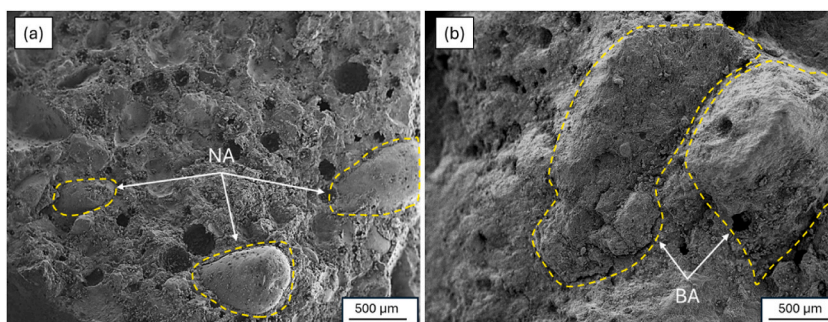


Fig. 7. SEM images for the microstructure cross-section of (a) 0BA and (b) 100BA mixtures after mechanical strength testing.

Table 2
CH content and bound water of the different LC3 samples with and without BA.

Mix ID	CH content [%]	Bound water [%]
CS	12.1	2.4
30BA	20.9	2.9
50BA	16	3
70BA	12.6	2.8
100BA	10.6	2.5

additional nucleation sites, allowing the paste matrix to provide better interlocking with BA particles and better bonding in the microstructure, as was shown in Fig. 7. Moreover, the values of bound water content also confirmed the development of more hydration products, which had higher values in the presence of BA. The bound water content is one of the most commonly used methods to monitor the hydration of cementitious materials. According to Huang et al. [22], the TG weight loss at the temperature range of 110–300 °C is due to the loss of the bound water from the chemical decomposition of the various hydration products, such as C-S-H and AFm. The mass loss associated with bound water was calculated and presented in Table 2. The bound water content was around 16–25 % higher than the control sample. That is due to the formation of additional hydration products due to the better hydration in the presence of BA, which increases the amount of chemically bound water content. The bound water increased when replacing up to 50 % of NA with BA. That indicates that the mixtures were able to bind more CH and produce more hydration products. Nevertheless, further increasing BA content to more than 50 % decreased the bound water content, indicating that 50 % was the threshold. However, it is still higher than that of the control sample. Moreover, it could be suggested that the activated clay minerals have already reacted during the hydration, and extra water for replacement levels above 50 % is not needed due to the low amount of kaolinite presented in excavated London clay. Even though, compressive strength didn't decrease at 70 % and 100 % replacement levels (see Fig. 6), which indicates that particle size and physical characteristics of BA are critical factors in strength growth.

3.1.3. Water absorption

The primary contributors to material deterioration necessitate both the presence and permeation of water within the mixture. Water presence could result in freeze-thaw harm to the cementitious mixture, while also transporting chlorides, sulphates, and other detrimental ions. Consequently, the absorption of the cementitious mixture profoundly impacts its durability and service life. The water absorption of LC3 mixtures with different BA content was investigated, and the results are presented in Fig. 8.

A clear trend can be observed from the results, where the water absorption increased with BA content. Interestingly, the LC3 mixture prepared with 30 % BA initially exhibited slightly higher water absorption percentages than the mix with NA. However, LC3-30BA exhibited water absorption percentages similar to the control sample after 60 min. Similarly, the LC3 mixture prepared with 50 % BA showed similar behaviour to that of 30 % BA, where the mix initially exhibited higher water absorption percentages, and after some time, the mixture's water absorption values reached values similar to those of the control sample. This trend was observed for all samples, where mixtures with BA after 5 min exhibited 10 %, 24 %, 33 %, and 48 % higher water absorption than OBA mixtures for 30, 50, 70 and 100 % BA content, respectively. The higher water absorption at the initial stages is attributed to the high capillary absorption of BA [52]. After 72 h, the LC3 mixture prepared with 30 and 50 % BA achieved similar water absorption values to OBA, while the 70BA mixture had around 2 % higher water absorption percentage than the reference mixture, which is negligible. On the other hand, 100BA achieved around 9 % higher water absorption value than the mixture prepared with NA. This behaviour could be

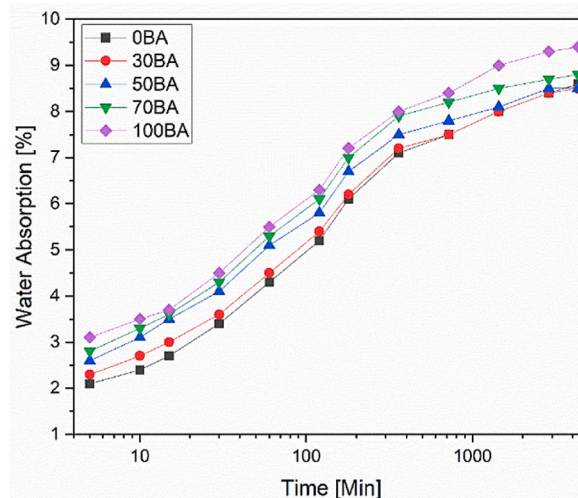


Fig. 8. Water absorption of LC3 mixtures with different BA content.

correlated with the development of additional hydration products in the mixtures containing BA, which could fill the pores and result in the development of a more densified and compacted microstructure, which could in turn decrease the porosity of the mixtures in the presence of BA. Thus, allowing the different mixtures to exhibit similar water absorption values.

Similar findings were reported elsewhere [53]. Dang et al. [53] reported that incorporating recycled BA to substitute 50 % of fine NA and compensating for BA water absorption resulted in around 30–40 % higher water absorption percentage than the control sample. Other studies observed higher water absorption percentages when incorporating BA to replace NA [54]. El-seidy et al. [54] found that incorporating BA to replace 50 % and 100 % of NA in two-part alkali-activated mortars resulted in 8 % and 25 % higher absorption values, respectively, than the control mixture. It is worth mentioning that the BA used in El-seidy et al. study has a water absorption capacity similar to the BA used in the current study. Similarly, Tavakoli et al. [55] reported the water absorption percentage increased by around 46 % when fully substituting sand in concrete with recycled BA. It should be noted that a limited comparison can be made due to the differences in BA characteristics and mix formulations. Compared to this work, the current study showed that incorporating different BA content has no or slight influence on the water absorption properties of the LC3 mixture, even for a 100 % replacement level. This behaviour could indicate the good compaction and the densified microstructure of LC3 mixes with different BA content (see Fig. 7).

3.1.4. Freeze-thaw (F-T) resistivity

Freeze-thaw (F-T) resistivity is one of the primary indicators to ascribe cementitious mixture durability, which is the ability to resist cyclic freezing and melting. During exposure to F-T cycles, the aqueous solution in the microstructure and capillary pores of the cementitious mixture transforms into ice and expands in the microstructure by around 9 % of its volume. This expansion causes unfrozen water to move into any available voids and eventually causes hydraulic pressure [56]. The matrix's irregular and non-homogenous pores may compensate for the hydraulic pressure to a certain level. However, once the pores are filled, the matrix may experience internal pressures due to the expansion of water upon freezing. When the pressures and forces induced from frozen water exceed the stress capacity of cementitious matrix, microcracks may be initiated and propagate throughout the mixture's microstructure, degrading the mixture's strength properties [57]. In addition, the expansion of the frozen water leads to rupturing and widening the pore structure, thus declining the strength properties of the cementitious mixture. Therefore, the deterioration of the properties depends mainly on the presence of free water in the system [58]. Hence, strength loss increases with the water absorption. Fig. 9 presents the compressive strength reduction after exposing the LC3 mixtures with different BA content to freeze-thaw cycles. Strength reduction was found to be 6.7 %–8.9 %. The strength reduction percentages of the different samples were comparable. Although, LC3 mixtures containing BA showed similar or higher water absorption percentages than the control sample (OBA), mixtures containing BA exhibited slightly lower strength reduction percentages compared to the OBA mix. This slightly better behaviour in the presence of BA can be associated with BA's porous microstructure, providing space to ease the induced pressure from forming ice. In addition, the microstructure of the LC3 mixture could be more densified in the presence of BA particles due to the good adhesion and interlocking between the paste and BA (see Fig. 7), which, in turn, increased the resistivity to freeze-thaw cycles. That is in line with the observations obtained by Ref. [59].

Huang et al. [22] reported that substituting NA with BA, while accounting for BA's water absorption, degraded cement mortars' properties. However, the current study findings indicate an opposite trend. The results presented in this work showed that the additional water included in the mix design to compensate for BA's water absorption was beneficial to the hydration of LC3, and resulted in developing a more densified mixture that exhibited better performance compared to that of the natural aggregates. This shows that compensating for BA's water absorption directly affects the mechanical strength, water absorption and freeze-thaw properties of the LC3 mixture for all replacement levels. However, above 50 % substitution level, the performance of the mixtures in all tests slightly decreased but stayed higher than that with NA. This suggests that the extra water for up to 50 % replacement level

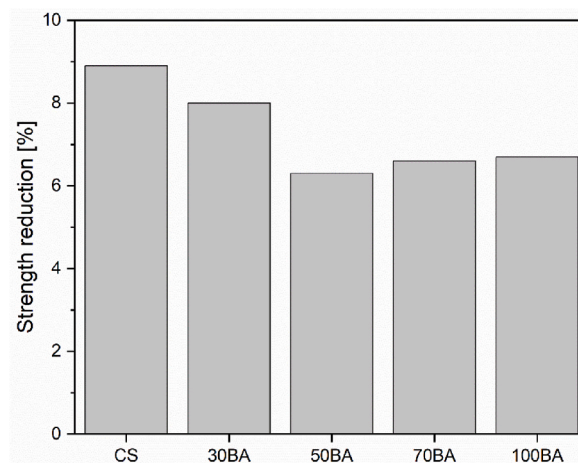


Fig. 9. Strength reduction percentage after exposure to freeze-thaw cycles.

has already facilitated the hydration process and consumption of the activated kaolinite clay in the reaction. However, because excavated London clay has low kaolinite content, adding more water for replacement levels above 50 % won't enhance internal curing but will instead reduce the quality of the mixture.

3.2. Printability and printing properties of LC3 system containing BA

3.2.1. Consistency modification of LC3 mixtures

The investigated LC3 systems with up to 50 % BA exhibited high flowability and slump height reduction due to the inclusion of extra water to compensate for BA particles' water absorption, as explained in Section 3.1.1. It should be noted that the authors excluded mixtures containing 70 % and 100 % BA from printing trials due to difficulties in their extrusion and to avoid clogging the nozzle of the hopper due to their high particle-to-particle packing. Hence, LC3 mixtures with up to 50 % BA content were considered for modification and 3D printing trials. It is well known that the high flowability of the mixtures would be beneficial for the mixture's extrudability. Nevertheless, high flowability would not allow the mixtures to retain their shape after extrusion, preventing the mixtures from forming the desired shape or object [60]. It is reported in the literature that VMA can reduce the workability of the cementitious mixture through two different mechanisms, i.e., flocculation and water retention [38]. It was reported that incorporating cellulose-derivative VMA can increase yield stress and plastic viscosity [37,61], which is beneficial for the extrudability and shape retention of the cementitious mixture. Hence, in this study, HPMC-based VMA was employed to modify the fresh properties of various mixtures, aiming to achieve a composition capable of retaining its shape. The optimum dosage of VMA was determined following a trial-based approach by incorporating different dosages and investigating its effect on the shape retention of each mixture. That was done by conducting printing trials to print a rectangular object consisting of four layers, as shown in Fig. 10, which shows the impact of various VMA dosages on the shape retention of an LC3 mixture prepared with 30 % BA content. It can be seen that incorporating 0.25VMA %-wt. improved the mixture's consistency and shape retention. However, it was not enough to allow the mix to gain adequate early strength to withstand the subsequent layers' weight, showing excessive deformation in the bottom layer, as seen in Fig. 10a. Increasing the VMA dosage to 0.4 wt% improved the shape retention of LC3-30BA significantly, allowing the print of four layers without showing any failure, as shown in Fig. 10b. Hence, this dosage was selected as the optimum for LC3-30BA. The same approach was considered for the other mixtures, and the optimum dosage was found to be 0.5 wt%, 0.4 wt% and 0.4 wt% for CS, 30BA and 50BA, respectively. According to Chen et al. [38], increasing VMA content to a certain level can enhance the ability of the extruded filaments to retain their shape. This was attributed to the relatively higher green strength development with increasing VMA dosage, in which the authors found that increasing VMA content from 0.12 wt% to 0.24 wt% and 0.48 wt% allowed the development of 5 times and 6 times higher green strength, respectively. Thus, the cementitious mixture can withstand more loads when depositing subsequent layers. Hence, in this study, the better shape retention is due to the higher green strength development with increasing VMA content. Moreover, when combined with PCE, HPMC-based VMA can significantly increase the thixotropy of cementitious mixture [62], which allows the mixture to achieve faster rigidification to sustain more stress, and thus retain the weight of the subsequent layers. Moreover, it can be seen that incorporating BA decreased the required VMA dosage to allow the mixtures to retain their shape, which is mainly due to the lower flowability and slump-height reduction with increasing BA content (see Fig. 5).

3.2.2. Printing properties

The buildability of the modified LC3 mixtures with and without BA was investigated through 3D printing a cylinder using a fixed amount of materials (8 Kg). It should be noted that further VMA modifications were considered when needed to find the optimum VMA dosage that makes the LC3 mixtures buildable without collapsing or failing. For instance, it was found that incorporating 0.4 % VMA was sufficient and allowed the mix to retain its shape during the printing trials for a rectangular object with four layers (see section 3.2.1). Nevertheless, 0.4 %-wt. VMA dosage for LC3-30BA was insufficient to allow the mixture to retain its shape in the buildability test. As a result, the cylinder collapsed because the bottom layers could not develop adequate early strength to sustain the load from the subsequent filaments, as shown in Fig. 11a. Hence, the VMA dosage of LC3-30BA was increased from 0.4 % to 0.5 %-wt., and the buildability of the mixture was re-assessed. 30BA mix containing 0.5 %-wt. was extruded and could retain the designated object shape, as shown in Fig. 11b. The better shape retention, as explained earlier, is attributed to the higher green strength in the presence of higher VMA dosage. Therefore, the modified VMA dosages are 0.5 %, 0.5 % and 0.4 % for CS, 30BA and 50BA, respectively.

Fig. 12 presents cylinders of the different modified mixtures, which contain 0.5 %, 0.5 %, and 0.4 % VMA for CS, 30BA, and 50BA,

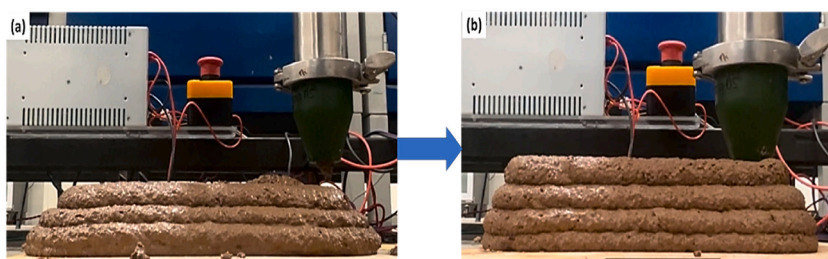


Fig. 10. Shape retention of LC3-30BA with (a) 0.25VMA %-wt. and (b) 0.4VMA %-wt.

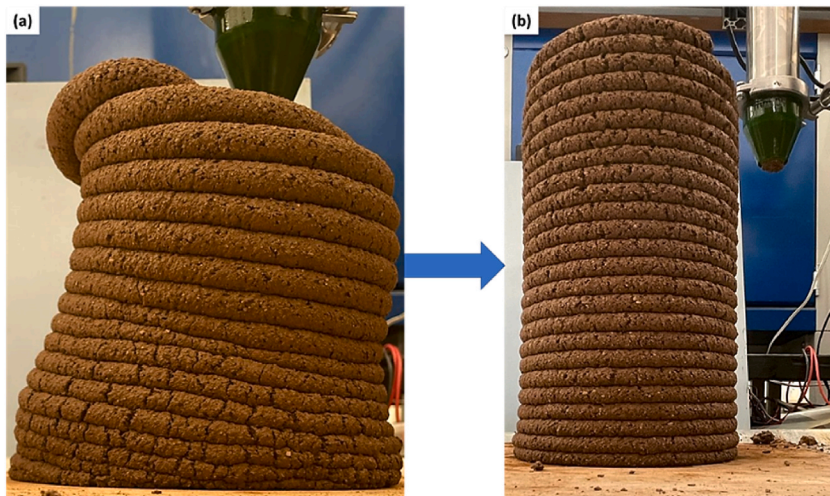


Fig. 11. Shape retention of 30BA using (a) 0.4 %-wt and (b) 0.5 %-wt. VMA dosages.

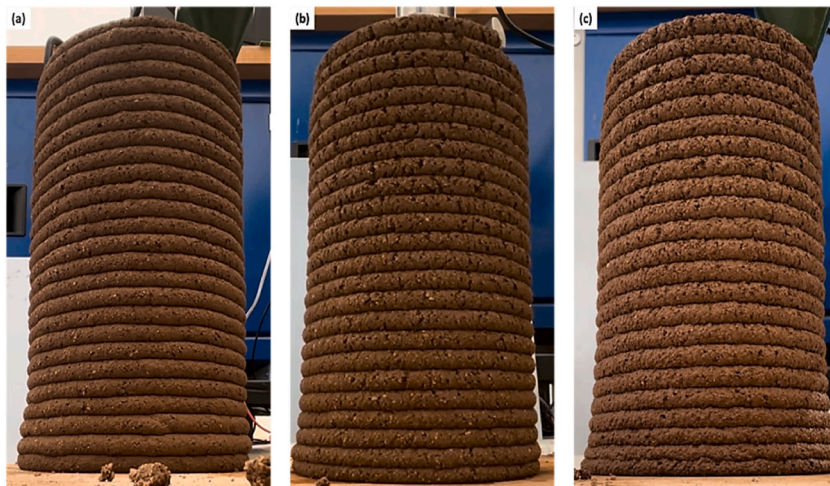


Fig. 12. Buildability of (a) CS, (b) 30BA, and (c) 50BA.



Fig. 13. Layers' printing quality of LC3 with NA (CS mix).

respectively. The buildability test was conducted until the fixed amount of fresh mixture was consumed, and the experimental height and layer number of the various mixtures were measured. All cylinders were printed without any discontinuity in printing or showing lateral deformation and achieved adequate shape and layer thickness, as seen in Fig. 12. Moreover, all cylinders had a comparable experimental height to the designated theoretical height, in which all layers maintained their designated thickness (i.e., 10 mm).

Although the different LC3 mixtures were modified to be buildable, incorporating BA to replace NA was found to cause some tears in the filaments. It should be noted that the printing parameters, such as printing speed and nozzle size, were kept constant for all the mixtures. The cylinders were examined more closely to understand the reason behind these tears better, as seen in Figs. 13–15. Some tears and voids were observed in all cylinders but increased when BA was incorporated. The cylinder prepared with CS mix showed fewer tears than those containing BA. Nevertheless, cracks immediately started showing on the outer surface of the filaments of CS mix, which could indicate that plastic shrinkage is taking place due to the fast evaporation of the free water in the system. On the other hand, no visible cracks were observed on the cylinders prepared with 30BA and 50BA mixes. This indicates that the water absorption of BA was more dominant over water evaporation, which would allow for maintaining the moisture within the layers and, thus, prevent plastic shrinkage from taking place. As discussed earlier, BA would start releasing water over time. Hence, once the available water in layers evaporated, BA would work on releasing some of the water it initially absorbed, preventing the cracks from occurring. Ge et al. [63] studied the influence of incorporating recycled fine BA to replace fine NA on the drying shrinkage properties of self-compacting concrete. They found the shrinkage to decrease with increasing the replacement level. Shrinkage, according to the authors, is mainly caused by the water loss in the reacted and hydrated binder components, which leads to capillary stress and surface tension. Using recycled fine BA with porous microstructure and high water absorption capacity could result in more effective internal curing [63]. That could explain the absence of cracks attributable to shrinkage in the presented study for the cylinder printed with BA. It should be noted that the shrinkage property isn't part of the current study, hence further research should be conducted. On the other hand, cylinders containing BA showed voids and tears on some of the layers. That could be related to BA's irregular particle shape that might have had its edge stuck (hanged) on the side of the nozzle's outlet, slightly delaying the extrusion and leading to form a small void in the extruded filament.

The modified mix formulations' open time was determined and presented in Table 3. The mixture prepared with NA had the highest open time, whereas the open time was reduced when incorporating BA. That is aligned with the authors' previous research [6], which found that incorporating BA up to 50 % significantly decreased the open time of one-part alkali-activated material. The reduction was attributed to the high water absorption of BA, which decreased the amount of free water in the mixture, however, it should be noted that no additional water was accounted for [6]. Based on authors' previous work, BA absorbs around 91 % of the maximum water absorption capacity of the BA particle within the first 30 min [6]. Although extra water for BA absorption was accounted for, BA absorbs most of it within the first 30 min, resulting in similar free water levels as in the CS mix with NA. Hence, it can be indicated that the decrease in open time could be related to the BA's particle morphology and coarser particle shape compared to that of NA, which increases the frictional resistance of the mixture during extrusion and, thus, lowers the open time of the LC3 mixtures with BA.

3.2.3. Mechanical properties of 3D printed LC3 mixtures

Fig. 16 presents flexural and compressive strength results of the different modified LC3 mixtures in cast and 3D printed. As per previous investigation, it is expected that VMA incorporation decreases the strength performance of LC3 mixtures [64]. Nevertheless, this study focuses on the impact of BA incorporation on the strength properties of the LC3 mixture. Moreover, it is expected that 3D-printed samples achieve lower strength performance than conventional cast samples. Similar to the results reported in section 3.1.2, LC3 containing BA maintained higher strength performances than the LC3 mix with NA. The highest strength performance was reported for LC3-50BA for cast and 3D printed samples, exhibiting around 28 % and 34 % higher flexural strength values for cast and 3D printed specimens, respectively, than the control sample. Similarly, 50BA exhibited around 55 % and 40 % higher compressive strength for cast and 3D printed specimens, respectively, compared to the control sample. Moreover, as expected, printed specimens exhibited slightly lower strength performance than the cast specimens, exhibiting around 16 %, 14 % and 14 % lower strength performance than the mould-cast specimens for CS, 30BA and 50BA, respectively. Rahul et al. [65] reported lower compressive strength performance for 3D printed specimens than the mould cast concrete. This was attributed to the weaker interfaces developed between the layers in 3D printed specimens with the increased porosities between filaments. Consequently, cracks may be initiated from these weak interfaces under load, causing a failure at lower stress values than the cast specimens. Hence, the lower mechanical strength behaviour of 3D printed samples in this study compared to cast could be attributed to the weaker interfacial bonding between the layers. Similarly, Ibrahim et al. [66] found that 3D printed LC3 specimens prepared using low-grade flash-calcined kaolinitic clay maintained slightly lower strength performance than the cast specimens, achieving around 22 MPa. This is similar to the results obtained in this study for the control specimen without BA incorporation. It should be noted that most studies investigated the flexural and compressive strength performance of mould cast LC3 specimens, and the literature lacks findings on the strength behaviour of 3D printed LC3. Hence, comparisons in this study are limited.

4. Conclusions

This study examined the influence of substituting natural aggregates with brick aggregates on the properties of limestone calcined clay cement with applications focused on cast and 3D printing processes aimed at producing medium to large-scale building blocks and structural elements. Recycled brick aggregates were incorporated to replace up to 100 % natural aggregates in the casting method, and their effect on fresh properties, mechanical strength, and durability were investigated. On the other hand, brick aggregate replacement levels were limited to 50 % in 3D printing applications due to the high particle-to-particle packing, which didn't allow for further



Fig. 14. Layers' printing quality of LC3-30BA mix.



Fig. 15. Layers' printing quality of LC3-50BA mix.

Table 3
Open time of the modified LC3 with NA, 30 % and 50 % BA.

Mix ID	CS-0.5 %-wt. VMA	30BA-0.5 %-wt. VMA	50BA-0.4 %-wt. VMA
Open time in minutes	80	60	55

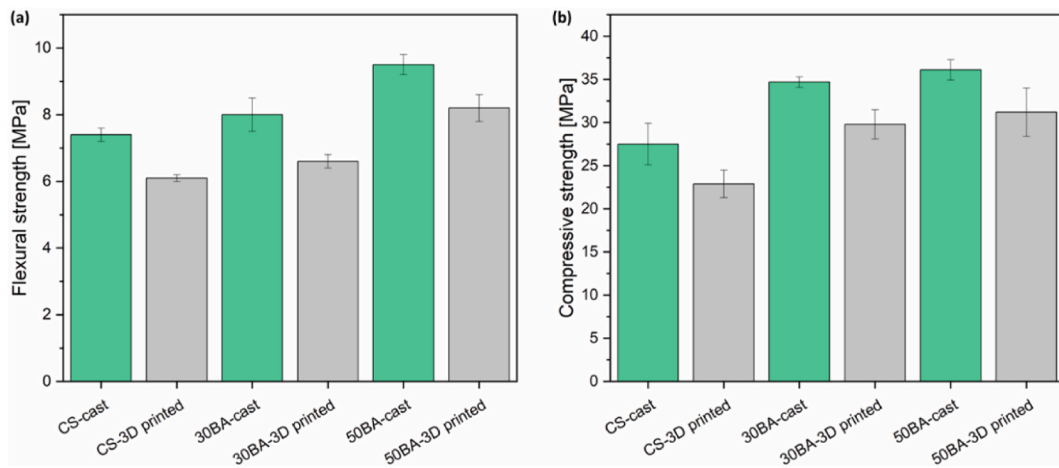


Fig. 16. (a) Flexural and (b) compressive strengths of cast and 3D printed modified CS, 30BA and 50BA.

replacements. The mixtures were further modified to retain their shape, and the impact of brick aggregates on buildability, printing quality, and mechanical strength was evaluated. Based on the findings of this study, the following conclusions can be made.

1. Brick aggregate inclusion leads to reduction of workability of the LC3 mixtures even though additional water was counted in the LC3 mix design due to BA's porous microstructure.
2. The incorporation of brick aggregates significantly enhances the strength performance of LC3 mixtures. Acting as an internal curing agent, it initially absorbs water and then releases it with ageing, facilitating further hydration. Furthermore, the angular shape and rough texture of brick aggregates also contribute to the improved mechanical strength behaviour of the LC3 mixtures, due to mechanical entanglements and interlocking.
3. The water absorption of LC3 mixtures initially increased with the increase in BA content. However, LC3 mixtures with up to 70 % BA showed similar water absorption percentages at 28 days. Moreover, the Incorporation of BA enhanced the resistivity of the LC3 mixture to freeze-thaw, indicating its potential benefits in terms of durability.
4. Shape retention of LC3 mixtures with and without BA was modified using VMA additives. Incorporating optimum dosages of VMA (i.e., 0.5 % for CS and 30BA, and 0.4 % for 50BA) allowed all mixtures to be buildable and achieve the designed shape.
5. Brick aggregate incorporation can overcome the torsions induced after depositing the layers. Nevertheless, some voids can occur due to the irregular/angular shape of BA.

Overall, this study revealed the suitability of repurposing end-of-life bricks into aggregates to improve the engineering and printing properties of low-carbon cementitious mixtures. However, additional research should be executed to investigate the effect of brick aggregates on the long-term performance of cementitious mixtures, including 90 days strength performance and resistivity under exposure to harsh environments. In addition, the impact of brick aggregates on shrinkage of LC3 should be investigated. More research should be conducted to study the influence of brick aggregates on the layers bonding of the 3D-printed cementitious mixtures. Moreover, additional research should be conducted to optimise the particle size distribution of BA and investigate different printing parameters to overcome extrusion-related issues. Furthermore, it would be interesting to investigate the effect of different printing speeds, nozzle geometry and mix modifications on the interfacial adhesion to overcome the reduction in compressive strength of 3D printed mixtures compared to cast.

CRediT authorship contribution statement

Yazeed A. Al-Noaimat: Writing – original draft, Methodology, Formal analysis, Data curation, Conceptualization. **Mehdi Chougan:** Writing – review & editing, Formal analysis, Data curation, Conceptualization. **Eslam El-Seidy:** Writing – review & editing, Data curation, Conceptualization. **Abdulrahman Albar:** Writing – review & editing, Methodology, Data curation. **Syed Hamidreza Ghaffar:** Writing – review & editing, Validation, Supervision, Methodology, Funding acquisition, Formal analysis, Conceptualization.

Declaration of competing interest

The authors declare that they have no known competing financial interests or personal relationships that could have appeared to influence the work reported in this paper.

Data availability

Data will be made available on request.

References

- [1] M.L. Nehdi, A. Marani, L. Zhang, Is net-zero feasible: systematic review of cement and concrete decarbonization technologies, *Renew. Sustain. Energy Rev.* 191 (2024) 114169, <https://doi.org/10.1016/j.rser.2023.114169>.
- [2] Y.A. Al-noaimat, T. Akis, Influence of cement replacement by calcinated kaolinitic and montmorillonite clays on the properties of mortars, *Arab. J. Sci. Eng.* (2023), <https://doi.org/10.1007/s13369-023-08041-y>.
- [3] Y.A. Al-noaimat, M. Chougan, M.J. Al-kheetan, O. Al-mandhari, W. Al-saidi, M. Al-maqbali, H. Al-hosni, S. Hamidreza, 3D printing of limestone-calcined clay cement : a review of its potential implementation in the construction industry, *Results Eng* 18 (2023) 101115, <https://doi.org/10.1016/j.rineng.2023.101115>.
- [4] Y.A. Al-noaimat, M. Chougan, M.J. Al-kheetan, M.H.N. Yio, H.S. Wong, S. Hamidreza, Upcycling end-of-life bricks in high-performance one-part alkali-activated materials, *Dev. Built Environ.* 16 (2023) 100231, <https://doi.org/10.1016/j.dibe.2023.100231>.
- [5] Y.A. Al-noaimat, S. Hamidreza, M. Chougan, M.J. Al-kheetan, A review of 3D printing low-carbon concrete with one-part geopolymer : engineering , environmental and economic feasibility, *Case Stud. Constr. Mater.* 18 (2023) e01818, <https://doi.org/10.1016/j.cscm.2022.e01818>.
- [6] Y.A. Al-noaimat, M. Chougan, A. Albar, S. Skibicki, K. Federowicz, M. Hoffman, D. Sibera, K. Cendrowski, M. Techman, Recycled brick aggregates in one-part alkali-activated materials : impact on 3D printing performance and material properties, *Dev. Built Environ.* 16 (2023), <https://doi.org/10.1016/j.dibe.2023.100248>.
- [7] C. Chen, R. Xu, D. Tong, X. Qin, J. Cheng, J. Liu, B. Zheng, L. Yan, Q. Zhang, A striking growth of CO₂emissions from the global cement industry driven by new facilities in emerging countries, *Environ. Res. Lett.* 17 (2022), <https://doi.org/10.1088/1748-9326/ac48b5>.
- [8] Supriya, R. Chaudhury, U. Sharma, P.C. Thapliyal, L.P. Singh, Low-CO₂ emission strategies to achieve net zero target in cement sector, *J. Clean. Prod.* 417 (2023) 137466, <https://doi.org/10.1016/j.jclepro.2023.137466>.
- [9] K. Scrivener, F. Martirena, S. Bishnoi, S. Maity, Calcined clay limestone cements (LC3), *Cement Concr. Res.* 114 (2018) 49–56, <https://doi.org/10.1016/j.cemconres.2017.08.017>.
- [10] J. Yu, D.K. Mishra, C. Hu, C.K.Y. Leung, S.P. Shah, Mechanical, environmental and economic performance of sustainable Grade 45 concrete with ultrahigh-volume Limestone-Calcined Clay (LCC), *Resour. Conserv. Recycl.* 175 (2021) 105846, <https://doi.org/10.1016/j.resconrec.2021.105846>.

- [11] N. Blouch, K. Rashid, I. Zafar, M. Ltifi, M. Ju, Prioritization of low-grade kaolinite and mixed clays for performance evaluation of Limestone Calcined Clay Cement (LC3): multi-criteria assessment, *Appl. Clay Sci.* 243 (2023) 107080, <https://doi.org/10.1016/j.clay.2023.107080>.
- [12] F. Avet, R. Snellings, A. Alujas, M. Ben, K. Scrivener, Development of a new rapid, relevant and reliable (R3) test method to evaluate the pozzolanic reactivity of calcined kaolinic clays, *Cement Concr. Res.* 85 (2016) 1–11, <https://doi.org/10.1016/j.cemconres.2016.02.015>.
- [13] H.G. Dill, Kaolin: soil, rock and ore: from the mineral to the magmatic, sedimentary and metamorphic environments, *Earth Sci. Rev.* 161 (2016) 16–129, <https://doi.org/10.1016/j.earscirev.2016.07.003>.
- [14] N. Blouch, K. Rashid, M. Ju, Exploring low-grade clay minerals diving into limestone calcined clay cement (LC3): characterization – Hydration – Performance, *J. Clean. Prod.* 426 (2023) 139065, <https://doi.org/10.1016/j.jclepro.2023.139065>.
- [15] T. Chompoorat, T. Thepumong, A. Khamplod, Improving mechanical properties and shrinkage cracking characteristics of soft clay in deep soil mixing, *Constr. Build. Mater.* 316 (2022) 125858, <https://doi.org/10.1016/j.conbuildmat.2021.125858>.
- [16] F. Kanavaris, A. Papakosta, F. Zunino, H. Pantelidou, A. Bernal, J. Szanser, A. Tsoumelekas, W. Wichmann, T. Burr-, Suitability of excavated London Clay from Tunnelling Operations as a Supplementary Cementitious Material and Expanded Clay Aggregate, (n.d.) 1–9.
- [17] A. Katz, D. Kulisch, Performance of mortars containing recycled fine aggregate from construction and demolition waste, *Mater. Struct. Constr.* 50 (2017) 1–16, <https://doi.org/10.1617/s11527-017-1067-x>.
- [18] S.M.A. Qaidi, Y.Z. Dinkha, J.H. Haido, M.H. Ali, B.A. Tayeh, Engineering properties of sustainable green concrete incorporating eco-friendly aggregate of crumb rubber: a review, *J. Clean. Prod.* 324 (2021) 129251, <https://doi.org/10.1016/j.jclepro.2021.129251>.
- [19] S.M.A. Qaidi, A.S. Mohammed, H.U. Ahmed, R.H. Faraj, W. Emad, B.A. Tayeh, F. Althoey, O. Zaid, N.H. Sor, Rubberized geopolymer composites: a comprehensive review, *Ceram. Int.* 48 (2022) 24234–24259, <https://doi.org/10.1016/j.ceramint.2022.06.123>.
- [20] T.R. da Silva, A.R.G. de Azevedo, D. Cecchin, M.T. Marvila, M. Amran, R. Fediuk, N. Vatin, M. Karelina, S. Klyuev, M. Szelag, Application of plastic wastes in construction materials: a review using the concept of life-cycle assessment in the context of recent research for future perspectives, *Materials* 14 (2021), <https://doi.org/10.3390/ma14133549>.
- [21] B.C. Lyu, L.P. Guo, X.P. Fei, J.D. Wu, R.S. Bian, Preparation and properties of green high ductility geopolymer composites incorporating recycled fine brick aggregate, *Cem. Concr. Compos.* 139 (2023) 105054, <https://doi.org/10.1016/j.cemconcomp.2023.105054>.
- [22] Q. Huang, X. Zhu, G. Xiong, C. Wang, D. Liu, L. Zhao, Recycling of crushed waste clay brick as aggregates in cement mortars: an approach from macro- and micro-scale investigation, *Constr. Build. Mater.* 274 (2021) 122068, <https://doi.org/10.1016/j.conbuildmat.2020.122068>.
- [23] Q. Liu, A. Singh, J. Xiao, B. Li, V.W. Tam, Workability and mechanical properties of mortar containing recycled sand from aerated concrete blocks and sintered clay bricks, *Resour. Conserv. Recycl.* 157 (2020) 104728, <https://doi.org/10.1016/j.resconrec.2020.104728>.
- [24] F. Debieb, S. Kenai, The use of coarse and fine crushed bricks as aggregate in concrete, *Constr. Build. Mater.* 22 (2008) 886–893, <https://doi.org/10.1016/j.conbuildmat.2006.12.013>.
- [25] J. Dang, J. Zhao, W. Hu, Z. Du, D. Gao, Properties of mortar with waste clay bricks as fine aggregate, *Constr. Build. Mater.* 166 (2018) 898–907, <https://doi.org/10.1016/j.conbuildmat.2018.01.109>.
- [26] Z. Zhang, Y. Choy, A. Arulrajah, S. Horpibulsuk, A review of studies on bricks using alternative materials and approaches, *Constr. Build. Mater.* 188 (2018) 1101–1118, <https://doi.org/10.1016/j.conbuildmat.2018.08.152>.
- [27] C. Lum, K. Hung, S. Poh, U.J. Alengaram, Potential use of brick waste as alternate concrete-making materials : a review, *J. Clean. Prod.* 195 (2018) 226–239, <https://doi.org/10.1016/j.jclepro.2018.05.193>.
- [28] Z. Ge, Y. Feng, H. Zhang, J. Xiao, R. Sun, X. Liu, Use of recycled fine clay brick aggregate as internal curing agent for low water to cement ratio mortar, *Constr. Build. Mater.* 264 (2020) 120280, <https://doi.org/10.1016/j.conbuildmat.2020.120280>.
- [29] G.M. Moelich, P.J. Kruger, R. Combrinck, A plastic shrinkage cracking risk model for 3D printed concrete exposed to different environments, *Cem. Concr. Compos.* 130 (2022) 104516, <https://doi.org/10.1016/j.cemconcomp.2022.104516>.
- [30] O. Olofinnade, J. Ogara, Workability, strength, and microstructure of high strength sustainable concrete incorporating recycled clay brick aggregate and calcined clay, *Clean. Eng. Technol.* 3 (2021) 100123, <https://doi.org/10.1016/j.clet.2021.100123>.
- [31] BS EN 197-1: Cement - Composition, Specifications and Conformity Criteria for Common Cements, (n.d.).
- [32] BS EN 12620, Aggregates for Concrete, 2013.
- [33] L. Zheng, Z. Ge, Z. Yao, Z. Gao, Mechanical properties of mortar with recycled clay-brick-powder, in: *Toward. Sustain. Transp. Syst.*, 2011, pp. 3379–3388.
- [34] H. Christen, G. van Zijl, W. de Villiers, The incorporation of recycled brick aggregate in 3D printed concrete, *Clean. Mater.* 4 (2022) 100090, <https://doi.org/10.1016/j.clema.2022.100090>.
- [35] Y. Briki, F. Avet, M. Zajac, P. Bowen, M. Ben Haha, K. Scrivener, Understanding of the factors slowing down metakaolin reaction in limestone calcined clay cement (LC3) at late ages, *Cement Concr. Res.* 146 (2021) 106477, <https://doi.org/10.1016/j.cemconres.2021.106477>.
- [36] F. Bektas, K. Wang, H. Ceylan, Effects of crushed clay brick aggregate on mortar durability, *Constr. Build. Mater.* 23 (2009) 1909–1914, <https://doi.org/10.1016/j.conbuildmat.2008.09.006>.
- [37] M. Palacios, R.J. Flatt, Working Mechanism of Viscosity-Modifying Admixtures, Elsevier Ltd, 2016, <https://doi.org/10.1016/B978-0-08-100693-1.00020-5>.
- [38] Y. Chen, S. Chaves Figueiredo, Z. Li, Z. Chang, K. Jansen, O. Çopuroğlu, E. Schlangen, Improving printability of limestone-calcined clay-based cementitious materials by using viscosity-modifying admixture, *Cement Concr. Res.* 132 (2020), <https://doi.org/10.1016/j.cemconres.2020.106040>.
- [39] M. Chougan, S. Hamidreza, B. Nematollahi, P. Sikora, T. Dorn, A. Albar, M.J. Al-kheetan, Effect of natural and calcined halloysite clay minerals as low-cost additives on the performance of 3D-printed alkali-activated materials, *Mater. Des.* 223 (2022) 111183, <https://doi.org/10.1016/j.matdes.2022.111183>.
- [40] BS EN 1015-3, Methods of Test for Mortar for Masonry- Part 3: Determination of Consistence of Fresh Mortar (By Flow Table), 1999 (n.d.).
- [41] BS EN 196-1, Methods of Testing Cement - Part 1: Determination of Cement, 2016 (n.d.).
- [42] Y.A. Al-noaimat, M. Sambucci, M. Chougan, E. El-seidy, S. Hamidreza, Sustainable Repurposing of Polyvinyl Chloride Waste as Aggregates in Limestone-Calcined Clay Cement, 2025, p. 491, <https://doi.org/10.1016/j.jclepro.2025.144862>.
- [43] BS 1881-122, Testing Concrete - Part 122: Method for Determination of Water Absorption, 2011 (n.d.).
- [44] PN-85/B-04500: Construction Mortars. Research of Physical and Strength Characteristics, Polish committee for standardization, Warsaw, Poland, 1985 (n.d.).
- [45] A. Bhowmick, S. Ghosh, Effect of synthesizing parameters on workability and compressive strength of Fly ash based Geopolymer mortar, *Int. J. Struct. Civ. Eng.* 3 (2012) 168–177, <https://doi.org/10.6088/ijcsr.201203013016>.
- [46] P.B. Cachim, Mechanical properties of brick aggregate concrete, *Constr. Build. Mater.* 23 (2009) 1292–1297, <https://doi.org/10.1016/j.conbuildmat.2008.07.023>.
- [47] S. Zhang, P. He, L. Niu, Mechanical properties and permeability of fiber-reinforced concrete with recycled aggregate made from waste clay brick, *J. Clean. Prod.* 268 (2020) 121690, <https://doi.org/10.1016/j.jclepro.2020.121690>.
- [48] Z. Xing, A.L. Beaucour, R. Hebert, A. Noumowe, B. Ledesert, Aggregate's influence on thermophysical concrete properties at elevated temperature, *Constr. Build. Mater.* 95 (2015) 18–28, <https://doi.org/10.1016/j.conbuildmat.2015.07.060>.
- [49] A.P.N. Siregar, M.I. Rafiq, M. Mulheron, Experimental investigation of the effects of aggregate size distribution on the fracture behaviour of high strength concrete, *Constr. Build. Mater.* 150 (2017) 252–259, <https://doi.org/10.1016/j.conbuildmat.2017.05.142>.
- [50] J. Sun, F. Zunino, K. Scrivener, Hydration and phase assemblage of limestone calcined clay cements (LC3) with clinker content below 50 %, *Cement Concr. Res.* 177 (2024) 107417 <https://doi.org/10.1016/j.cemconres.2023.107417>.
- [51] R. Hay, L. Li, K. Celik, Shrinkage , hydration , and strength development of limestone calcined clay cement (LC3) with different sulfation levels, *Cem. Concr. Compos.* 127 (2022) 104403, <https://doi.org/10.1016/j.cemconcomp.2021.104403>.
- [52] Y. Li, J. Shen, H. Lin, J. Lv, S. Feng, J. Ci, Properties and environmental assessment of eco-friendly brick powder geopolymer binders with varied alkali dosage, *J. Build. Eng.* 58 (2022) 105020, <https://doi.org/10.1016/j.job.2022.105020>.

- [53] J. Dang, J. Zhao, S. Dai, S. Zhao, Durability and microstructural properties of concrete with recycled brick as fine aggregates, *Constr. Build. Mater.* 262 (2020) 120032, <https://doi.org/10.1016/j.conbuildmat.2020.120032>.
- [54] E. El-seidy, M. Chougan, Y.A. Al-noaimat, M.J. Al-kheetan, H. Ghaffar, The impact of waste brick and geo-cement aggregates as sand replacement on the mechanical and durability properties of alkali – activated mortar composites, *Results Eng* 21 (2024) 101797, <https://doi.org/10.1016/j.rineng.2024.101797>.
- [55] D. Tavakoli, P. Fakharian, J. De Brito, Mechanical properties of roller-compacted concrete pavement containing recycled brick aggregates and silica fume, *Road Mater. Pavement Des.* 23 (2022) 1793–1814, <https://doi.org/10.1080/14680629.2021.1924236>.
- [56] A. Allahverdi, M. Mahdi, B. Rasht, K.M. Anwar, M. Lachemi, Cold Regions Science and Technology Resistance of chemically-activated high phosphorous slag content cement against freeze – thaw cycles, *Cold Reg. Sci. Technol.* 103 (2014) 107–114, <https://doi.org/10.1016/j.coldregions.2014.03.012>.
- [57] E. El-seidy, M. Sambucci, M. Chougan, Y.A. Ai-noaimat, M.J. Al-kheetan, I. Biblioteca, M. Valente, S. Hamidreza, Alkali activated materials with recycled unplasticised polyvinyl chloride aggregates for sand replacement, *Constr. Build. Mater.* 409 (2023) 134188, <https://doi.org/10.1016/j.conbuildmat.2023.134188>.
- [58] W. Wang, Z. Zhong, X. Kang, X. Ma, Physico-mechanical properties and micromorphological characteristics of graphene oxide reinforced geopolymer foam concrete, *J. Build. Eng.* 72 (2023) 106732, <https://doi.org/10.1016/j.jobe.2023.106732>.
- [59] Y. Ji, Z. Pei, W. Xu, Z. Li, Y. Li, Y. Jia, Deterioration performance analysis of recycled brick concrete subjected to freezing and thawing effect, *Case Stud. Constr. Mater.* 20 (2024) e02722, <https://doi.org/10.1016/j.cscm.2023.e02722>.
- [60] Y.W.D. Tay, Y. Qian, M.J. Tan, Printability region for 3D concrete printing using slump and slump flow test, *Composites, Part B* 174 (2019) 106968, <https://doi.org/10.1016/j.compositesb.2019.106968>.
- [61] K.H. Khayat, N. Mikanovic, Viscosity-enhancing Admixtures and the Rheology of Concrete, Woodhead Publishing Limited, 2012, <https://doi.org/10.1533/9780857095282.2.209>.
- [62] H. Bessaies-bey, K.H. Khayat, M. Palacios, W. Schmidt, N. Roussel, Viscosity modifying agents : key components of advanced cement-based materials with adapted rheology, *Cement Concr. Res.* 152 (2022) 106646, <https://doi.org/10.1016/j.cemconres.2021.106646>.
- [63] Z. Ge, Y. Feng, H. Yuan, H. Zhang, R. Sun, Z. Wang, Durability and shrinkage performance of self-compacting concrete containing recycled fine clay brick aggregate, *Constr. Build. Mater.* 308 (2021) 125041, <https://doi.org/10.1016/j.conbuildmat.2021.125041>.
- [64] Y. Chen, S.C. Figueiredo, Ç. Yalçinkaya, O. Çopuroğlu, F. Veer, E. Schlangen, The effect of viscosity-modifying admixture on the extrudability of limestone and calcined clay-based cementitious material for extrusion-based 3D concrete printing, *Materials* 12 (2019) 9–12, <https://doi.org/10.3390/ma12091374>.
- [65] A.V. Rahul, M. Santhanam, H. Meena, Z. Ghani, Mechanical characterization of 3D printable concrete, *Constr. Build. Mater.* 227 (2019) 116710, <https://doi.org/10.1016/j.conbuildmat.2019.116710>.
- [66] K.A. Ibrahim, G.P.A.G. van Zijl, A.J. Babafemi, Influence of limestone calcined clay cement on properties of 3D printed concrete for sustainable construction, *J. Build. Eng.* 69 (2023) 106186, <https://doi.org/10.1016/j.jobe.2023.106186>.